Indian Journal of Pure & Applied Physics
Vol. 50, May 2012, pp. 339-346

Study of structural property of *n*-type indium antimonide thin films

S R Vishwakarma*, A K Verma, R S N Tripathi, S Das & Rahul

Department of Physics & Electronics, Dr R M L Avadh University, Faizabad 224 001, India

*E-mail: srvfzb@rediffmail.com

Received 2 September 2011; revised 4 January 2012; accepted 12 March 2012

In present study, the *n*-type indium antimonide (InSb) thin films of thickness 300 nm were deposited on glass substrate at room temperature under the high vacuum ~10^{-5} torr using starting materials. The starting materials have been prepared under vacuum ~10^{-5} torr in vacuum coating unit using indium (99.999%) and antimony (99.999%) metal powder as source materials with various non-stoichiometric composition as $In_{1-x}Sb_x$ ($0.2 < x < 0.4$). The Energy Dispersive Analysis of X-rays (EDAX) measurement provides the information of chemical composition (In/Sb) in thin films. X-ray diffraction studies of starting materials and thin films confirmed the formation of InSb with polycrystallinity and orientation of crystallites along the (111) and (220) planes. The surface morphological study of thin films by scanning electron microscope reveals the crystalline nature which was found to be in good agreement with the XRD crystallinity analysis. The particle size (D), dislocation density (δ) and strain (ε) have been evaluated using XRD data for the starting materials and thin films. It is observed from X-ray diffraction patterns and scanning electron micrographs that particle size, dislocation density and strain are changing with composition ratio (In/Sb) in starting materials and their thin films.

Keywords: InSb thin films, Particle size, Dislocation density, Strain, Lattice parameter

1 Introduction

In recent years, the growth of InSb thin films has attracted attention as a potential material for infrared detectors and high speed devices because of its small band gap. The III-V semiconductors, due to their structure, conventionally play a major role in scientific research and its applications. Among the III-V binary compound semiconductors, indium antimonide shows *n*-type and *p*-type semiconductivity, polycrystallinity and melts at 525°C. It is a narrow band gap semiconductor with an energy band gap[1–3] of 0.17 eV at 300 K and 0.23 eV at 80 K. In *n*-type indium antimonide (anion vacancy), the electrons have high electron mobility (80,000 cm^2/Vs) due to their smaller effective mass. Similarly in *p*-type InSb (cation vacancy), the holes have the mobility 1250 cm^2/Vs. Therefore, InSb is a material available for magnetic-field sensing devices such as Hall sensor and magnetoresistors[4], speed-sensitive sensors[5] and magnetic sensors[6]. The infrared detectors fabricated with *n*-type InSb thin films are sensitive between 3-5 μm wavelengths[7]. These *n*-type InSb thin films can also be used as bio-sensor to detect the bacteria. Many reports are available on the growth of InSb thin films using different deposition techniques such as molecular beam epitaxy[8], metal organic chemical vapour deposition[9] and vacuum evaporation[10]. The non- stoichiometry in thin films of indium antimonide created during their deposition. The anion vacancies i.e. indium enriched exhibit *n*-type semiconductivity and the cation vacancies exhibit *p*-type semiconductivity due to excess of antimony. The aim of present study is to fabricate *n*-type indium antimonide thin films, therefore, prepared indium enriched non-stoichiometric InSb powder with different composition of indium and antimony. This is a novel method to create controlled amount of non-stoichiometry in thin films. We have fabricated *n*-type InSb thin films by electron beam evaporation technique using starting materials which have controlled non-stoichiometric composition. The electron beam evaporation technique is more suitable among physical evaporation because during the deposition, materials come into vapour state without changing in liquid state. Finally, we have optimized the composition of starting materials on the basis of structural parameters.

2 Experimental Details

2.1 Preparation of starting materials

Indium and antimony metal powders of purity 99.999% have been purchased from Alfa-Aesar Ltd, USA. To prepare the non-stoichiometric starting materials for fabrication of *n*-type indium antimonide thin films, first we take different amount of In (indium) and Sb (antimony) metal powder using

composition $In_{1x}Sb_x$ ($0.2 \le x \le 0.4$. For each composition, the indium and antimony metal powder were mixed by grinding with mortar rod and then mixed powder was heated at 50°C in vacuum unit (Hind Hivac Company Ltd, India) using molybdenum boat under a vacuum 2×10^{-5} torr for ten hours and cooled up to room temperature in the same vacuum condition. This cooled mixture material again grinded with mortar rod and heated in same vacuum condition with enhanced temperature. This process was repeated five times with different temperature some higher than previous to each composition for formation of crystalline *n*-type InSb through solid reaction.

2.2 Preparation of InSb thin films

Before deposition of thin films, borosil glass substrates were boiled in chromic acid for two hours, then washed using distilled water and rinsed by acetone. They were finally cleaned with distilled water in ultrasonic bath and dried at 423 K in oven. The *n*-type InSb thin films of thickness 300 nm were grown on glass substrate at temperature 300 K. For this, prepared starting materials were taken in the graphite crucible and targeted by beam of electrons in vacuum (~10^{-5} torr), where the vacuum system equipped with liquid nitrogen trap. The source materials kept at a distance of 125 mm from the substrate holder. The deposition rates (0.5-18) nm/s were adjusted by changing the filament current of electron beam gun power supply. The thickness and deposition rate were measured by digital film thickness monitor (VICO, DTM-10) using a quartz crystal sensor set at 6 MHz.

2.3 Chemical analysis of thin films

The chemical compositional analysis of some representative thin films has been studied by Energy Dispersive Analysis of X-rays (EDAX) technique using scanning electron microscope Carl Zeiss EVO40 series from Advance instrument research facility, Jawaharlal Nehru University, New Delhi.

2.4 Structural measurement of starting materials and thin films

The X-Ray diffraction pattern of starting materials obtained by X-Ray Diffractometer (Rigaku D/max-2200) using Cukα_1 radiation of wavelength 1.5404 Å at 40 kV and 20mA in scanning angle between 20° to 90° at the Centre of Science & Nanotechnology, University of Allahabad, Allahabad, India. The X-Ray diffractogram of *n*-type InSb thin films have been obtained by Philips Analytical X-Ray diffractometer (PW-3710) using Cukα_1 radiation (λ=1.5418Å) with Ni-filter at 35 kV and 30 mA in scanning angle between 20° to 70° at Department of Physics, JMI University, New Delhi, India. The scanning electron micrograph (SEM) of *n*-type InSb thin films have been taken by Scanning Electron Microscope (Technai G2-300 kV) operated at 20 kV at Centre of Science & Nanotechnology, Allahabad University, Allahabad, India.

2.5 Optical measurement of thin film

Optical transmittance of *n*-type InSb thin film fabricated from starting material has composition $In_{0.66}Sb_{0.34,}$ is recorded using Fourier transform infrared spectrophotometer (FTIR) model No.Jasco/4100 in wave number range 1000-3000 cm^{-1} from Department of Physics, The M S University, Vadodara (Gujarat). From the transmission data, the absorption coefficient (α) is calculated for deposited thin film in the region of strong absorption using the relation[11]:

$$\alpha = 1/d\{\ln(1/T)\} \quad \ldots(1)$$

where α is absorption coefficient at particular wavelength, T the transmittance at same wavelength and d is film thickness.

The direct band gap of thin film is calculated by using Tauc relation[12]:

$$\alpha h\nu = A(h\nu - E_g)^n \quad \ldots(2)$$

where $h\nu$ is Photon energy, E_g is band gap, A is constant, n = ½ for direct band gap material.

3 Results and Discussion

The X-Ray Diffractogram of starting materials are shown in Fig. 1-10. In diffractogram, large number of diffraction peaks of InSb with different (*h k l*) planes

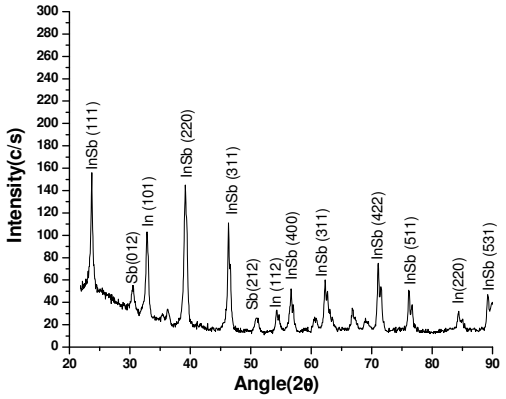

Fig. 1 — X-ray diffraction of starting material of composition $In_{0.60}Sb_{0.40}$

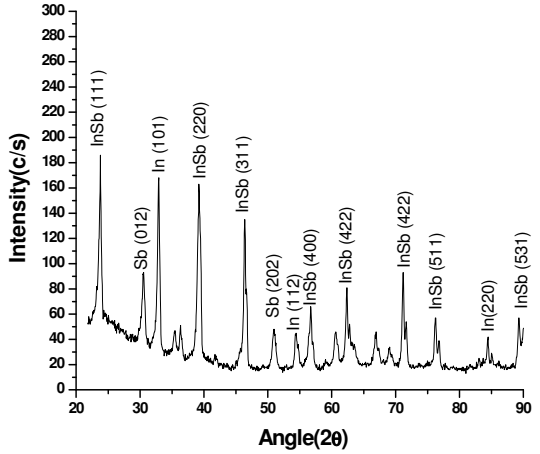

Fig. 2 — X-ray diffraction of starting material of composition $In_{0.62}Sb_{0.38}$

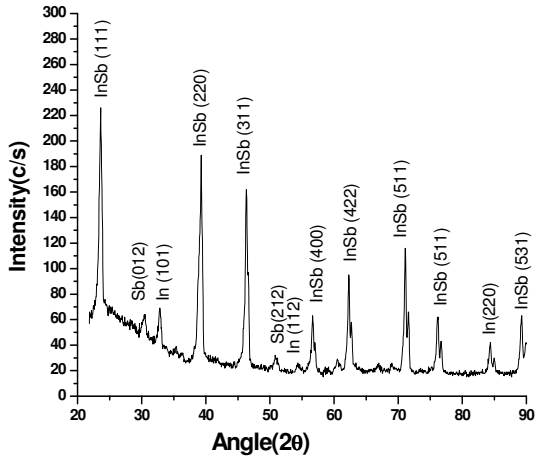

Fig. 3 — X-ray diffraction of starting material of composition $In_{0.64}Sb_{0.36}$

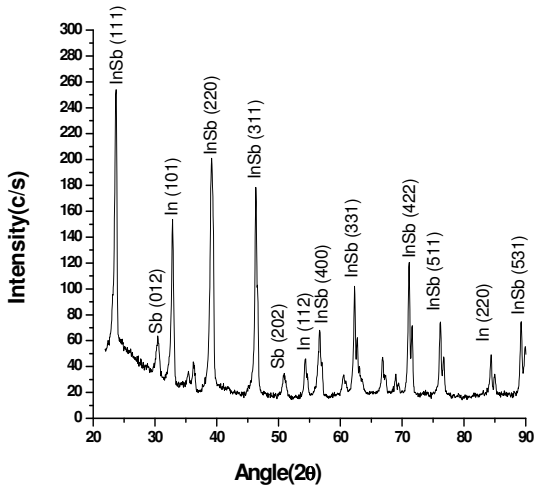

Fig. 4 — X-ray diffraction of starting material of composition $In_{0.66}Sb_{0.34}$

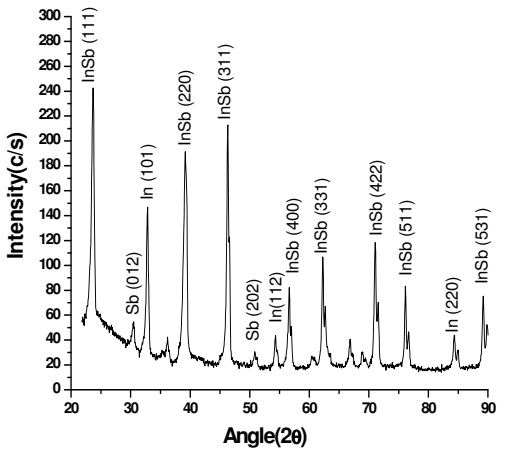

Fig. 5 — X-ray diffraction of starting material of composition $In_{0.68}Sb_{0.32}$

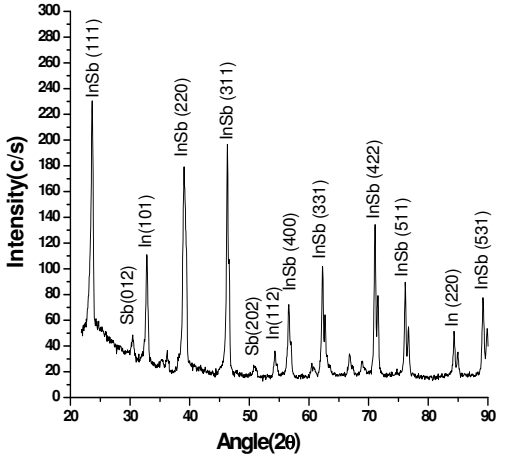

Fig. 6 — X-ray diffraction of starting material of composition $In_{0.70}Sb_{0.30}$

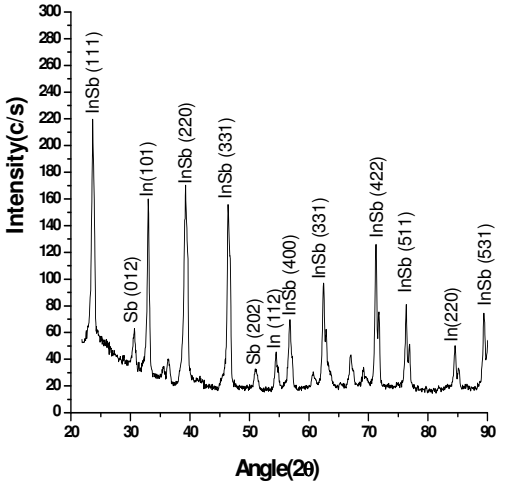

Fig. 7 — X-ray diffraction of starting material of composition $In_{0.72}Sb_{0.28}$

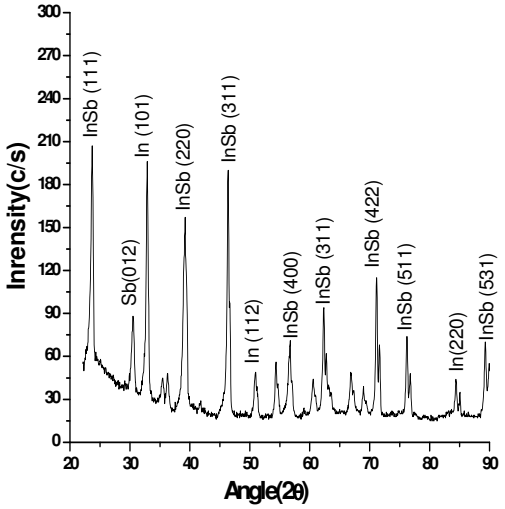

Fig. 8 — X-ray diffraction of starting material of composition $In_{0.74}Sb_{0.26}$

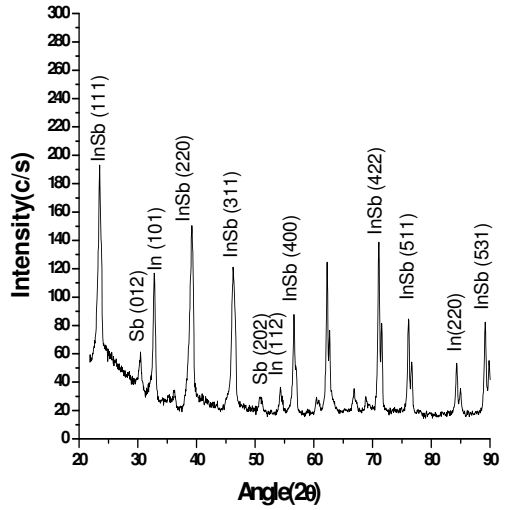

Fig. 9 — X-ray diffraction of starting material of composition $In_{0.76}Sb_{0.24}$

of high intensity are present but few peaks of In and Sb with less intensity are also present. Thus, X-ray diffraction patterns confirmed the formation of InSb with polycrystalline nature in starting materials.

The X-ray diffractogram of *n*-type thin films, prepared by using starting materials, are shown in Figs 11-15. These patterns confirmed the polycrystalline nature of the *n*-InSb thin films. From the XRD patterns, it has been observed that the crystallites have zinc blende structures with orientation along the (111) and (220) planes. The intensity of diffraction peaks of indium antimonide change with increase of the composition ratio of In/Sb in starting materials. The diffraction peaks of indium

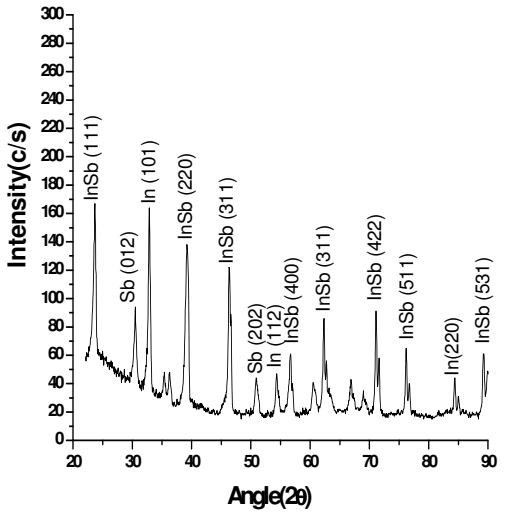

Fig. 10 — X-ray diffraction of starting material of composition $In_{0.78}Sb_{0.22}$

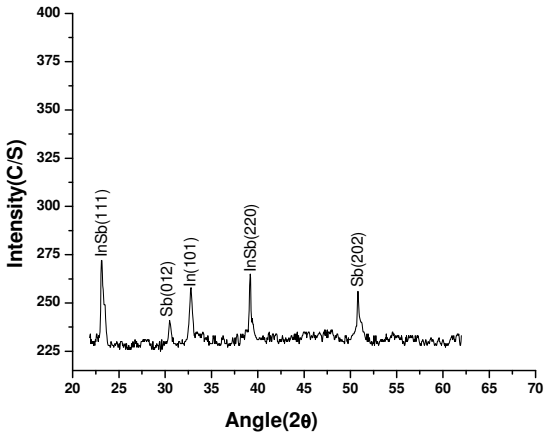

Fig. 11 — X-ray diffraction of *n*-type InSb thin films prepared using starting materials of composition $In_{0.60}Sb_{0.40}$

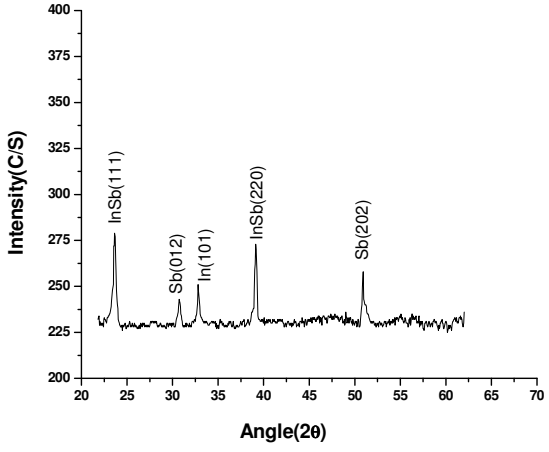

Fig. 12 — X-ray diffraction of *n*-type InSb thin films prepared using starting materials of composition $In_{0.62}Sb_{0.38}$

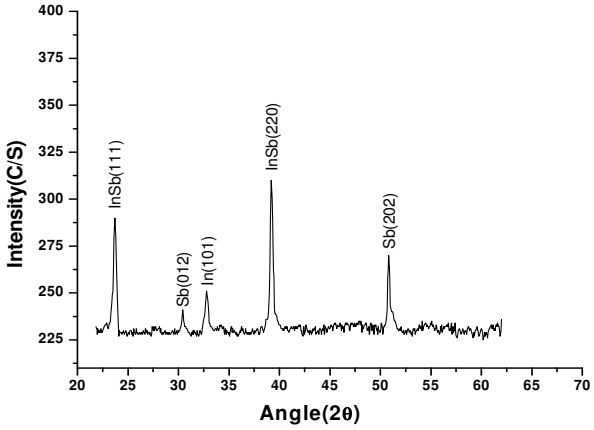

Fig. 13 — X-ray diffraction of *n*-type InSb thin films prepared using starting materials of composition $In_{0.64}Sb_{0.36}$

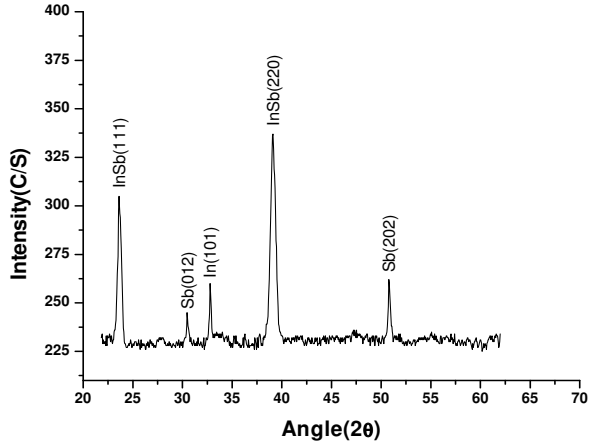

Fig. 14 — X-ray Diffraction of *n*-type InSb thin films prepared using starting materials of composition $In_{0.66}Sb_{0.34}$

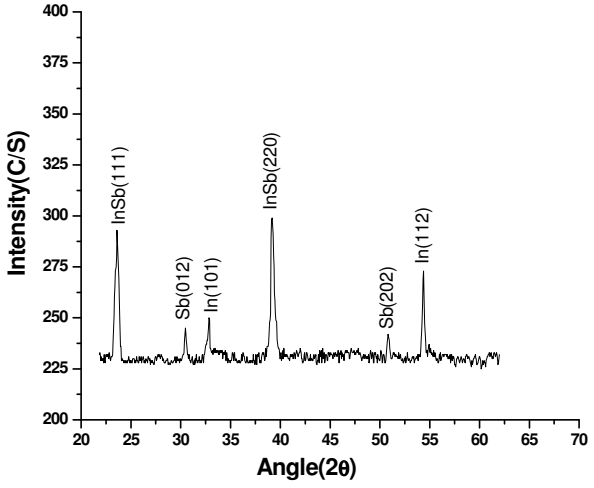

Fig. 15 — X-ray diffraction of *n*-type InSb thin films prepared using starting materials of composition $In_{0.68}Sb_{0.32}$

and antimony also appeared. The crystallites in a polycrystalline material normally have a different orientation plane from its neighbours[10], a similar result has also been observed in present study. The orientation of the crystallites is randomly distributed with respect to some selected frame of reference. The diffraction patterns of *n*-type InSb thin films are highly oriented along (111) and (220) planes in the present investigation, a similar planes and results have been also observed by other investigators Tahar[10], Senithilkumar[13] and Singh[15].

The experimental inter planer space "*d*" value recorded by diffractometer for starting and thin films, their corresponding (*h k l*) planes obtained with the help of Joint Committee on Powder Diffraction Standard (JCPDS card no.PDF#06-0208) data are given in Table 1.

The crystallite size (*D*) of the starting materials and *n*-type InSb thin films are calculated by Debye Scherrer's formula[11] for (111) and (220) planes, as given in Tables 2 and 3.

$$D = 0.94\lambda / \beta \cos\theta \qquad \ldots(3)$$

where β is the FWHM of diffraction peak, λ is wavelength of used X-ray and θ is diffraction angle.

The strain value (ε) for *n*-type InSb thin films calculated for (111) and (220) planes by use of following relation and presented in Table 3.

$$\beta = (\lambda / D\cos\theta) - \varepsilon \tan\theta \qquad \ldots (4)$$

The dislocation density (δ) defined as the length of dislocation lines per unit volume of the crystal and its value calculated with help of crystallite size (*D*) for the starting materials and *n*-type thin films, using the following formula[11] and given in Tables 2 and 3.

$$\delta = 1 / D^2 \qquad \ldots (5)$$

Table 1 — Experimental and standard '*d*' values of *n*-type InSb thin films and their corresponding (*h k l*) plane

S. No	Diffraction angle (2θ) deg.	Observed '*d*' value (Å)	Standard '*d*' value (Å)	(*h k l*) plane corresponding to InSb
1.	23.64	3.751	3.740	(111)
2.	39.17	2.287	2.290	(220)
3.	56.66	1.619	1.620	(400)
4.	46.38	1.952	1.953	(311)
5.	76.33	1.247	1.247	(511)

Table 2 — Structural parameters of starting materials

Composition ratio (In/Sb) in starting materials	(111) plane			(220) plane		
	Grain size (D) (nm)	Dislocation density (δ)$\times10^{16}$ lin/m^2	Lattice parameter (a)$\times10^{-10}$ m	Grain size (D) (nm)	Dislocation density (δ)$\times10^{16}$ lin/m^2	Lattice parameter (a) $\times10^{-10}$ m
$In_{0.60}Sb_{0.40}$	7.22	1.92	6.517	6.75	2.19	6.495
$In_{0.62}Sb_{0.38}$	7.63	1.72	6.515	6.94	2.08	6.493
$In_{0.64}Sb_{0.36}$	8.05	1.54	6.514	7.20	1.93	6.490
$In_{0.66}Sb_{0.34}$	8.42	1.41	6.512	7.56	1.75	6.487
$In_{0.68}Sb_{0.32}$	8.14	1.51	6.514	7.27	1.89	6.490
$In_{0.70}Sb_{0.30}$	7.75	1.66	6.515	6.87	2.12	6.493
$In_{0.72}Sb_{0.28}$	7.33	1.86	6.517	6.61	2.29	6.496
$In_{0.74}Sb_{0.26}$	6.95	2.07	6.519	6.30	2.52	6.498
$In_{0.76}Sb_{0.24}$	6.61	2.29	6.520	6.00	2.78	6.498
$In_{0.78}Sb_{0.22}$	6.27	2.54	6.522	5.73	3.05	6.501

Table 3 — Structural parameters of n-type InSb thin films

Composition Ratio(In/Sb) in starting materials%	Composition Ratio(In/Sb) in thin film%	(111) plane				(220) plane			
		Grain size (nm)	Dis. Density $\times10^{15}$ line/m^2	Lattice parameter x 10^{-10} m	Strain (ε) $\times$ 10^{-3} lin^{-2} m^{-4}	Grain size (nm)	$D$is. Density $\times10^{15}$ line/m^2	Lattice parameter ($\times10^{-10}$ m)	Strain (ε)$\times10^{-3}$ lin^{-2} m^{-4}
$In_{60}Sb_{40}$	58.48/39.58	11.08	8.15	6.520	4.49	10.93	8.37	6.498	2.79
$In_{62}Sb_{38}$	61.17/37.83	11.98	6.97	6.519	4.16	11.34	7.78	6.495	2.68
$In_{64}Sb_{36}$	63.35/35.45	12.70	6.20	6.517	3.94	12.88	6.03	6.493	2.34
$In_{66}Sb_{34}$	65.92/33.83	13.97	5.12	6.515	3.20	14.20	4.96	6.490	2.14
$In_{68}Sb_{32}$	66.73/31.37	12.92	5.99	6.519	3.90	13.44	5.54	6.495	2.28

The lattice parameter 'a' calculated for crystals of starting materials and n-type InSb thin films with the help of (111), (220) planes and following equation[11], are presented in Tables 2 and 3.

$$d = a/(h^2 + k^2 + l^2)^{1/2} \quad \ldots(6)$$

where d is interplanner space.

The chemical compositional analysis data of InSb thin films are presented in Table 3. From Table 3, it can be seen that the composition of indium and antimony in thin film and starting materials are nearly equal and have minute difference approximately one per cent. This difference decreases with increase of indium in starting material and found to be minimum for $In_{0.66}Sb_{0.34}$ composition of starting material.

It has been observed from Tables 2 and 3 that the crystalline size (D) of crystallite, lattice parameters(a) and dislocation density (δ) in starting materials and thin films are changing with composition ratio (In/Sb) in starting materials and orientation of the planes. The strain value (ε) observed in thin films is also varying with composition ratio in starting materials and orientation of the planes. The big grain (8.42 nm), large lattice parameters (6.512×10^{-10} m) and low dislocation density (1.41×10^{16} line/m^2) have been observed for (111) plane in $In_{0.66}Sb_{0.34}$ composition of starting materials. While big grain (14.20 nm), large lattice parameters (6.490×10^{-10} m) and low dislocation density (4.96×10^{15} line/m^2) have been observed for (220) plane in n-type InSb thin films prepared with composition $In_{0.66}Sb_{0.34}$ of starting materials. The minimum strain (2.14×10^{-3} lin^{-2} m^{-4}) in InSb thin films prepared with $In_{0.66}Sb_{0.34}$ composition of starting materials.

The grain size and lattice parameter increase but dislocation density decreases when thin films prepared using same composition of starting materials with change of orientation of the plane. The increase in grain size of crystallites in thin films may be due to decrease in strain value or coalescence of small crystallites[10]. Since dislocation density and strains are the manifestation of dislocation network in the films. The observed structural parameters of n-type InSb thin films in present study are found to be good agreement with the results observed by other investigators[10,13,14]. The low values of the dislocation density and strain in thin films for (220) planes

indicate the formation of high-quality thin films[13,15] of *n*-type InSb.

Scanning electron micrographs (SEM) have been used for the analysis of surface morphology *n*-type InSb thin films. The SEM pictures of *n*-InSb films on glass substrate are shown in Figs 16-20. It is cleared from micrographs that the deposited *n*-InSb films are homogenous, without cracks or holes, well covered to the glass substrate and the size of crystallites is of the order of nanometers which are confirmed by X-ray measurement. The variation of crystallites size with composition ratio in starting materials is also confirmed by scanning electron microscope patterns.

The indium antimonide (InSb) is a direct band gap material, therefore, variation of $(\alpha h\nu)^2$ with photon energy for InSb thin films of thickness 300 nm fabricated with $In_{0.66}Sb_{0.34}$ composition starting

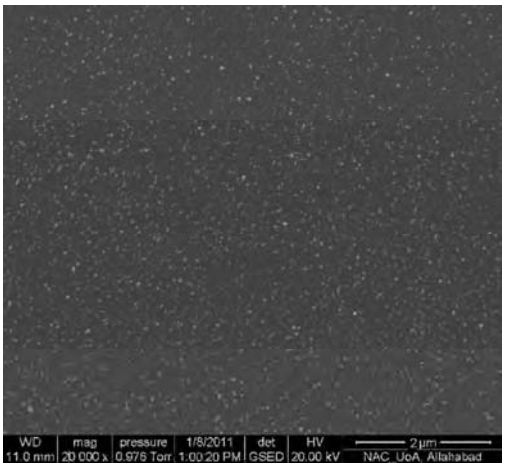

Fig. 16 — SEM of n-type InSb thin films prepared from starting materials of composition-$In_{0.60}Sb_{0.40}$

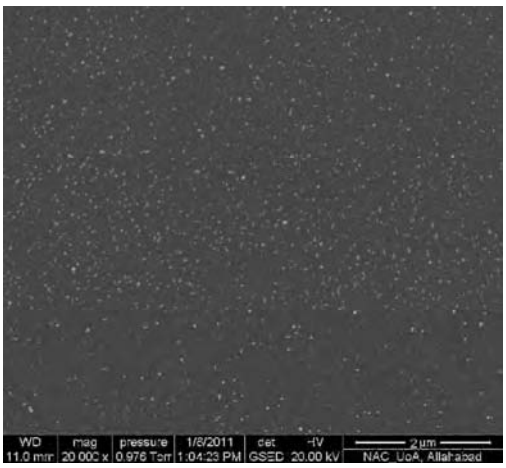

Fig. 17 — SEM of n-type InSb thin films prepared from starting materials of composition-$In_{0.62}Sb_{0.38}$

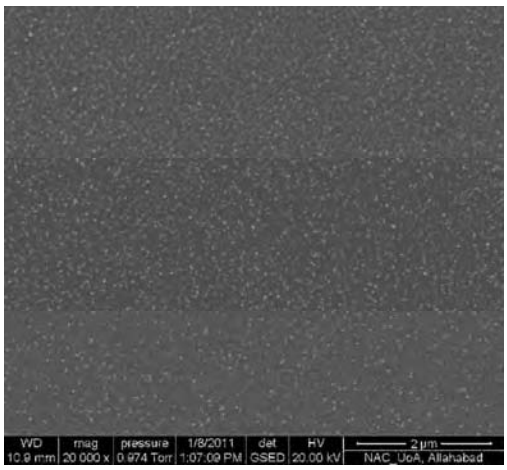

Fig. 18 — SEM of *n*-type InSb thin films prepared from starting materials of composition-$In_{0.64}Sb_{0.36}$

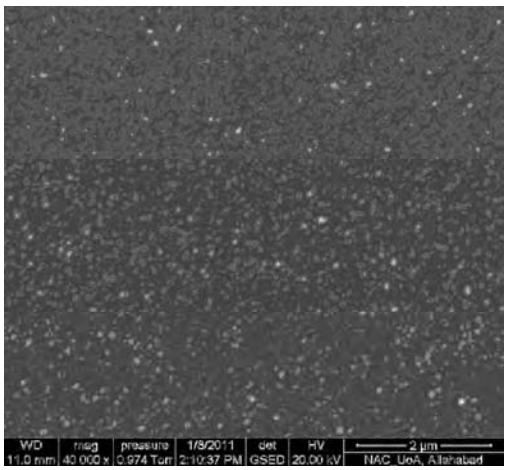

Fig. 19 — SEM of *n*-type InSb thin films prepared from starting materials of composition-$In_{0.66}Sb_{0.34}$

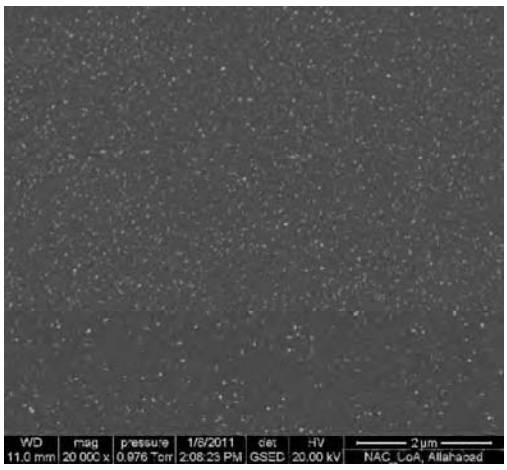

Fig. 20 — SEM of *n*-type InSb thin films prepared from starting materials of composition-$In_{0.68}Sb_{0.32}$

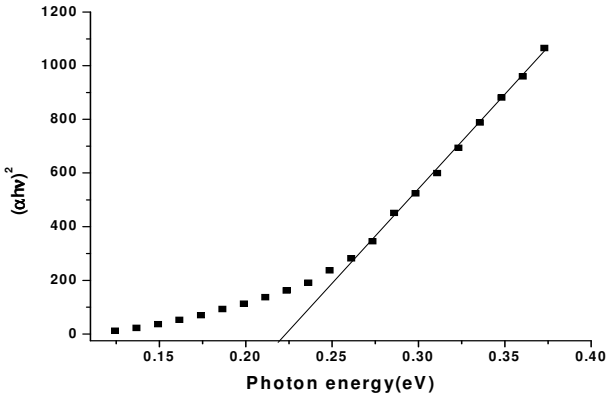

Fig. 21 — Photon energy versus $(\alpha h\nu)^2$ of *n*-InSb thin film fabricated composition of starting material $In_{0.66}Sb_{0.34}$

materials at room temperature is shown in Fig. 21. Extrapolation of straight-line portion to $(\alpha h\nu)^2 = 0$ axis gives the value of direct band gap. It is found that the direct band gap 0.22 eV and band gaps observed in present investigation are found to be similar with observed by other investigators[1,3,15].

4 Conclusions

Non-stoichiometric InSb compound (anion vacancy) as starting materials of polycrystalline nature with zincblende crystal structure with (111) and (220) plane of orientation have been prepared using molybdenum boat in vacuum for deposition of *n*-type InSb thin films. The *n*-type InSb thin films have been deposited on glass substrate at room temperature of 300 nm thickness by electron beam evaporation technique with use of starting materials. These deposited films are polycrystalline and have zinc blende structure with same plane of orientation but (220) plane is preferred. A grain growth noticed with increase in composition ratio of indium/antimony in starting materials and thin films. Scanning electron microscopic study confirmed the smooth surface of films. The particle size (D), dislocation density (δ) and strain (ε) change with increase of composition ratio (In/Sb) in starting material and thin films. The composition $In_{0.66}Sb_{0.34}$ is better for deposition of *n*-type InSb thin films because the films have better structural parameters, low direct band gap and minimum deviation of composition during deposition of thin films.

Acknowledgement

The financial support has been provided by U.P, Council of Science & Technology, Lucknow and University Grant Commission, New Delhi. Authors are highly thankful to Prof. K. Singh, Department of Physics & Electronics, Dr. R. M. L Avadh University, Faizabad for useful discussion. Authors are also thankful to Prof. Avinash Chandra Pondey, Allahabad University, Allahabad and Head, Department of Physics, Jamia Milia Islamia University, New Delhi for providing SEM and XRD facilities.

Reference

1 Mangal R K & Vijay Y K, *Bull Mater Sci*, 30 (2007) 117.
2 Mangal R K, Triapthi B, Singh M, Vijay Y K & Rais A, *Indian J Pure & Appl Phys*, 45 (2007) 987.
3 Mangal R K, Vijay Y K, Avatshi D K & Shekhar B R, *Indian J Engng & Mater Sci*, 14 (2007) 253.
4 Heremans J, Partin D L& Thrush C M, *Semi Sci Tech,* 8 (1993) 424.
5 Carpenter M K & Verbrugge M W, *J Mater Res*, 9 (1994) 2584.
6 Okamoto A, Yoshida T, Muramatsu S & Shibasaki I, *J Cryst Growth*, 201(1999) 765.
7 Udayshankar N K & Bhat H L, *Bull Mater Sci*, 24 (2001) 445.
8 Zhang T, Clowes S K, Debnath M, Bennett A, Roberts C, Harris J J & Stradling R A, *Appl Phys Lett*, 84 (2004) 22.
9 Gaskill D K, Stauf G T & Bottka N, *Appl Phys Lett* 58 (1991) 1905.
10 Taher M A, *Daffodil International University Journal of Science and Technology*, 2 (2007) 39.
11 Mehta C,Abass J,Saini G & Tripathi S, *Chalcogenide letter,* 11 (2007)133.
12 Singh M & Vijay Y K, *Indian J Pure & Applied Phys* 42 (2004) 610.
13 Senithilkumar V, Venkatachalam S, Viswanathan C, Gopal S, Mangalraj D & Wilson K C, *Cryst Res Technol*, 40 (2005) 573.
14 Tomisu M, Inoue N & Yasuaka Y, *Vacuum*, 47 (1996) 239.
15 Singh S, Lal K, Srivastava A K, Sood K N & Kishor R, *Indian J Engng & Mater Sci*, 14 (2007) 55.